CASL-U-2015-0016-000

Advanced Calibration and Validation of a Mechanistic Model of Subcooled Boiling Two-Phase Flow

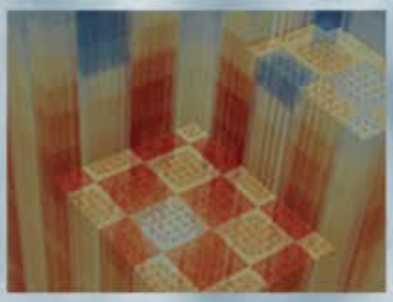

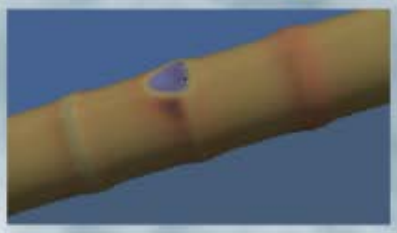

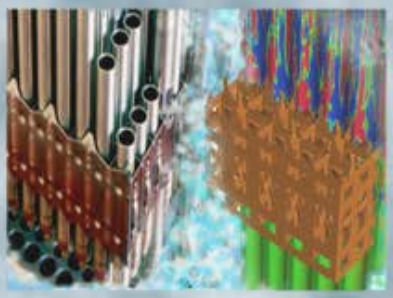

Anh Bui, Idaho National Laboratory
Brian Williams, Los Alamos National Laboratory
Nam Dinh, North Carolina State University

April 6, 2014

U.S. DEPARTMENT OF ENERGY | Nuclear Energy

CASL-U-2015-0016-000

Proceedings of ICAPP 2014
Charlotte, USA, April 6-9, 2014
Paper 14257

Advanced Calibration and Validation of a Mechanistic Model of Subcooled Boiling Two-Phase Flow

Anh Bui[1], Brian Williams[2], Nam Dinh[3,*]
[1]*Idaho National Laboratory (INL)*
[2]*Los Alamos National Laboratory (LANL)*
[3]*North Carolina State University (NCSU)*
[*] *Address: 3145 Burlington Laboratories, Raleigh, NC 27695-7909*
Tel:(919)515-5421, Fax:(919)515-5115, Email: ntdinh@ncsu.edu

Abstract – *In this work, an advanced approach to calibration and validation of typical multiphysics multiscale models of nuclear thermal hydraulics is proposed, which employs statistical modeling methods and Bayesian inference. The approach is then applied to calibrate a two-phase flow model, which describes the complex physics of subcooled boiling flow (SBF) using a conservation laws-based Eulerian-Eulerian multi-fluid model and a mechanistic model of wall evaporation. Various empirical closure models describing microscopic wall evaporation physics, e.g. nucleation, bubble growth and departure, etc., and related parameters are simultaneously calibrated. It is demonstrated in this study that the proposed model calibration/validation approach allows the integration of data of different types (e.g. 0D/1D, from both integral and separate effect tests) and of different qualities (defined by relevancy, scalability, and uncertainty) in the calibration/validation process. Moreover, the new approach allows to take into consideration the effects of data uncertainty and to quantify prediction uncertainty.*

I. INTRODUCTION

Reactor thermal hydraulics is a relatively complex multi-scale/multi-physics physical process which involves heat-mass transports by single-/multi-phase flows, inter-phase interactions, turbulence, complex flow geometry-flow momentum exchange, wall evaporation, etc. Thermal hydraulic codes used in nuclear reactor analysis employ a range of modeling approaches. At large scale, the phenomenology of two-phase transports is normally described using the multi-fluid continuum formulation and a system of mass, momentum and energy conservation equations derived for each phase. At smaller scales, many wall-flow and inter-phase physics, e.g. interfacial forces, wall evaporation, etc., are happening, which can only be described in an approximation manner using various empirical/semi-empirical closure models. To a large extent, the accuracy of (and uncertainty in) model predictions depends on the appropriate calibration of these closure models.

Calibration and validation of such complex multi-scale/physics modeling hierarchy are traditionally conducted in a sequential manner, in which empirical/semi-empirical submodels are first calibrated and validated using separate-effect test (SET) data and the whole model is then validated against integral-effect test (IET) data (Fig. 1). The approach suffers from several short-comings such as: (i) inability to account for data quality (relevancy, scalability, uncertainty) and quantify prediction uncertainty; (ii) difficulty in determination of the submodels which contribute the most to prediction error/uncertainty; (iii) inability to update a model incrementally based on newly available data.

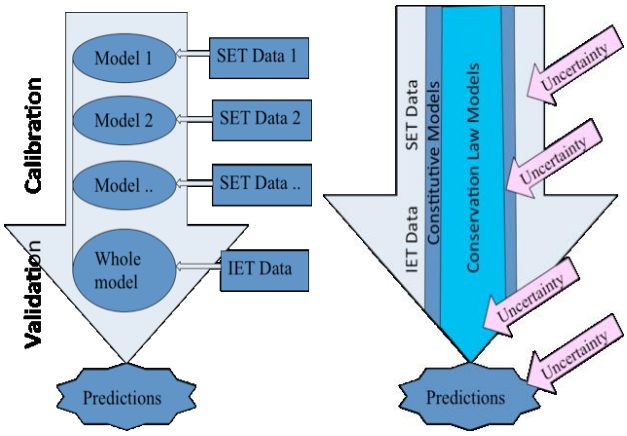

Fig. 1. Traditional model calibration/validation versus "total model-data integration" approaches

A new approach is presented in this work which offers a better use of various (heterogeneous) data in a comprehensive calibration/validation of complex physical

models. The approach illustratively shown in Fig.1 and capable of addressing all above shortcomings is based on statistical modeling methods and Bayesian inference. Initially proposed in [1], the approach is extended in this work to demonstrate its capability in assimilation of heterogeneous data in comprehensive model calibration and validation.

II. THERMO-HYDRAULIC MODEL OF TWO-PHASE FLOWS WITH SUBCOOLED BOILING

The phenomenology of two-phase flow transports is commonly described using a continuum formulation with both continuous and dispersed phases assumed to be interpenetrating continua collocating in space. Such a description of two-phase flows can be mathematically formulated using averaging techniques and the laws of mass, momentum, and energy conservations. The system of conservation equations for each phase (flow field) can therefore be derived, which forms the backbone of the popular Eulerian-Eulerian approach to modeling of two-phase flows [2].

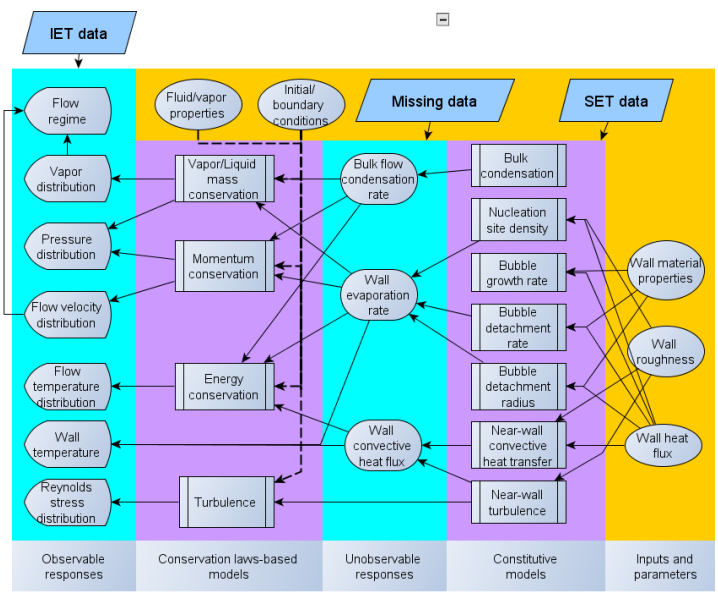

Fig. 2. Hierarchy of subcooled boiling flow model and validation data [1].

In addition to the macro-physics of two-phase flow transports described by the above-mentioned system of conservation equations, many physical interactions are happening at the meso- and micro-scales which include: (i) momentum and heat-mass exchanges between phases (at the phase interfaces), e.g. drag, lift, virtual mass forces; bubble deformation, coalescence, and breakup; bubble condensation, (ii) mechanical and thermal interactions on the heating wall, e.g. nucleation, bubble growth/departure, wall heat transfer governed by both convective heat transfer and evaporation, etc. Due to the substantial differences between these physics and average flow in space and time scales and the deficiency/lack of knowledge/understanding about them, the effects of such small-scale physics on the average flow are normally approximated using the so-called closure models, which are commonly derived from separate-effect-test (SET) data. The development and application of empirical/semi-empirical closure models and correlations can be seen as a data assimilation/integration process, which is an essential part of the modeling. Uncertainty in modeling of subcooled flow boiling mostly arises from the necessary use of these data-dependent closure models, which are normally the targets of the whole model calibration/validation exercise.

II.A. Drift-Flux Two-Phase Flow Model

A simplified one-dimensional (1D) drift-flux model [2][3] was used in this study for simulation of heat-mass transports by subcooled boiling flows. This model can be derived from the two-fluid 6-equation model with the relative velocity between phases defined analytically. As a result, the total number of equations reduces by one and the resulted equation system allegedly becomes more well-posed and easier to be solved. Only bubbly flow regime was considered in this work which helped to reduce uncertainty associated with the use of empirical flow regime transition maps.

II.B. Constitutive/Closure Models

Thermo-fluid dynamics of subcooled boiling flows is dominated by heat transfer at the heating wall which in turn is governed by wall evaporation. Such a small-scale phenomenon is only one of many others, which can not be directly described by the main conservation equations and are normally approximated by various closure/constitutive submodels, which are very different in their applicability and scalability. For instance, many such submodels have been derived based on experimental data obtained at low pressure and simple flow conditions making them inapplicable to reactor high pressure and complex flow conditions.

In this study, the physics of wall evaporation was modeled in a "mechanistic" manner with the evaporation rate defined based on (i) active nucleation site density, N_a , (ii) bubble departure frequency, f_d, and (iii) bubble departure diameter, D_d. Bubble departure diameter was determined by Tolubinsky & Konstanchuk's formulation [6] which is expressed in the general form as follows

$$D_d = d_0 \exp\left(-\Delta T_{sub}/\Delta T_{ref}\right) \quad (1)$$

where ΔT_{sub} and ΔT_{ref} denote the local and reference fluid subcoolings, respectively, and d_0 is the bubble size scaling parameter.

Bubble departure frequency was defined by Cole's correlation $f_d \sim 1/\sqrt{D_d}$ [7].

Active nucleation site density was computed using the Lemmert & Chawla's correlation [8]:

$$N_a = \bar{N}_a (\Delta T_w)^{1.805} \quad (2)$$

with $\bar{N}_a$ indicating the reference nucleation site density and ΔT_w being the local wall superheat.

It is notable that above correlations are commonly used in commercial CFD software, such as CFX-4/5 and Star-CFD/CCM+.

Heat from the wall was then considered to be transferred to flow via three mechanisms: namely single-phase turbulent convection, surface quenching, and evaporation [9].

III. VALIDATION DATA AND ADVANCED MODEL CALIBRATION BASED ON STATISTICAL MODELING AND BAYESIAN INFERENCE

III.A. Validation Data for SBF Model

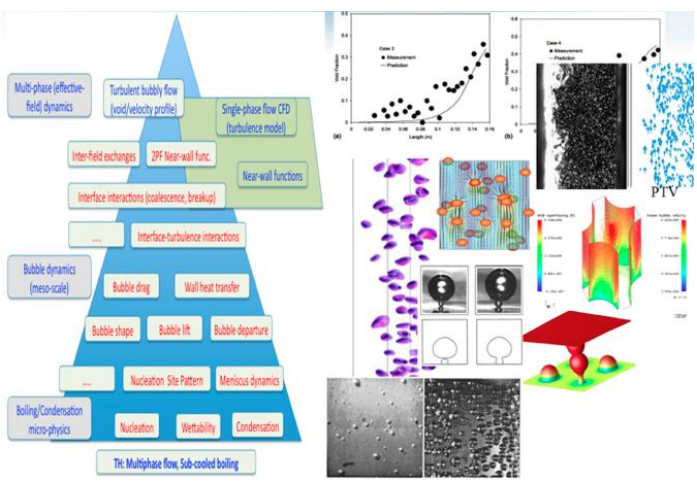

Fig. 3. Pyramid of subcooled-boiling flow physics and related validation data (including experimental measurements and Direct-Numerical Simulation (DNS) simulations).

Validation data are heterogeneous. For subcooled boiling flows, data can be in the form of macroscopic distributions of phase temperature, velocity, volume fraction, and microscopic measurements of bubble size, nucleation pattern, bubble growth dynamics, etc. Experimental data can be obtained for a wide range of system configurations (large/small, simple/complex geometries) and conditions (high/low pressure, flow rate, heat flux, etc.). Quality of such data in application to calibration and validation of reactor analysis codes has therefore to be quantified. Validation data quality can be assessed based on their relevancy, scalability and uncertainty [4]. Data uncertainty is of special interest since it will propagate to parameter uncertainty in the calibration process as shown later. Data uncertainty is defined not only by the sensitivity and accuracy of measurement techniques and sensors, but also the methods of data derivation (from raw measurement signals).

Direct Numerical Simulations (DNS) based primarily on first-principle modeling of two-phase flow phenomena and employing various interface tracking methods (ITMs) [5] can be used as "data" sources for calibration and validation of lower-fidelity subcooled boiling flow model presented in this work.

Heterogeneous measurement data were used in this calibration and validation. Data used in this case study calibration/validation included 1D axial distributions of void fraction and fluid temperature together with measurements of bubble departure diameter.

Experimental data on axial void fraction distribution obtained in Bartolomej et al.'s experiments (TABLE I) [10], which are scaled relatively well with the PWR conditions, were used in the calibration. The pipe diameter and flow rate for all these data were constant at 24 mm and 890 kg/(m^2 s), respectively. These data were obtained for upward bubble two-phase flow with forced convection subcooled boiling heat transfer. The error of void fraction measurement was estimated to be less than 0.01 in absolute value. Since there was no measurement of axial fluid temperature distribution in Bartolomej et al.'s experiments, these data were generated from simulations conducted for the conditions listed in TABLE I.

TABLE I
Conditions of experimental data by Bartolomej et al.'s [10] used in the calibration.

Experiment	Pressure p, MPa	Inlet ΔT_{sub}, K	Heat flux, kW/m^2
1	3.0	23.9	380
2	3.0	47.0	790
3	4.5	26.4	380
4	4.5	52.4	790

Data on bubble departure diameter were also artificially generated based on Tolubinsky & Konstanchuk's data (Fig. 4) with some scaling applied to take into account the dependence of bubble departure size on pressure (i.e. smaller bubble departure diameter with higher pressure). The scaling was based on the correlation

$$\frac{D_d}{D_{d,0}} = 1.27 \times 10^{-3} \left(\frac{\Delta\rho}{\rho_g}\right)^{0.9}$$

given in the work by Kocamustafaogullari [11].

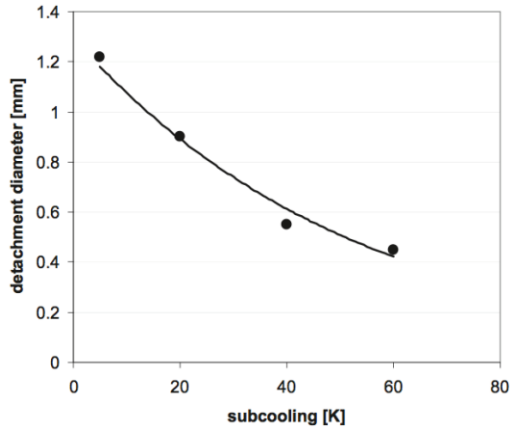

Fig. 4. Measured bubble departure sizes by Tolubinsky & Konstanchuk (dots).

III.B. Technical Approach For Subcooled Boiling Flow Model Calibration and Validation

Parameters subjected to calibration in this study include d_0, ΔT_{ref}, and $\bar{N}_a$. Bayesian calibration of these parameters was carried out with use of the LANL Gaussian Process Models for Simulation Analysis (GPM/SA) toolbox [12]. The calibration process was conducted in the following steps (Fig. 5):

1. Generating simulation "data" needed for the construction of a model surrogate with DAKOTA [13];

2. Constructing a model surrogate using a combination of Principal Component Analysis (PCA) [14], process convolution technique [15], and Gaussian processes (GPs);

3. Conducting Bayesian calibration with Markov chain Monte Carlo (MCMC) method.

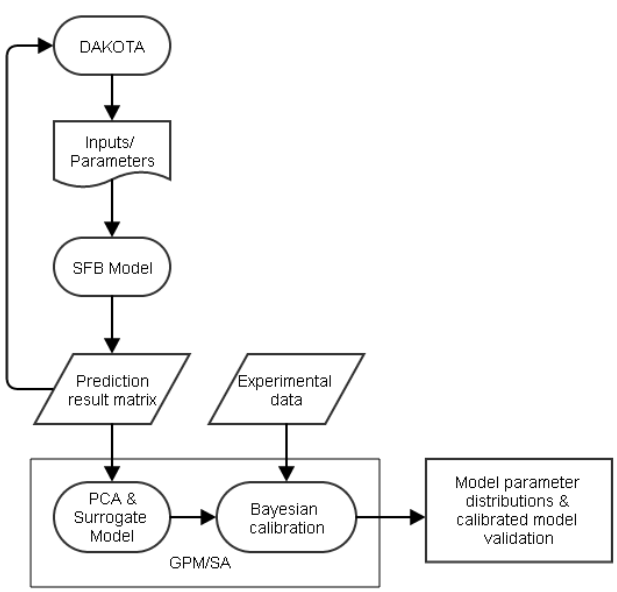

Fig. 5. The workflow of subcooled boiling flow model calibration and validation.

300 simulation predictions were generated with the runs controlled by DAKOTA. The inputs and calibration parameters were sampled with LHS (Latin Hypercube Sampling) in the ranges shown in TABLE II. The outputs of interest included one-dimensional distributions of fluid temperature and void fraction along the pipe as well as local wall superheat and corresponding bubble departure diameter. All these outputs and their correlations were then used in the surrogate construction.

TABLE II
Ranges of inputs and calibration parameters.

p, MPa	Inlet ΔT_{sub}, K	Heat flux, kW/m^2
3-5	20-55	360-800
d_0, mm	ΔT_{ref}, K	$\bar{N}_a$, 1/m^2
0.1-0.8	30-60	(1-10)×10^5

Given the large amount of outputs, the construction of a model surrogate started with a dimensionality reduction using PCA. PCA employs a limited set of linearly uncorrelated principal components (PC) to "explain" a majority of variance in the observations (simulation outputs). As shown in Fig. 6, 99.9% of variance in the 300 predictions of fluid temperature and void fraction can be explained with the first six major principal components.

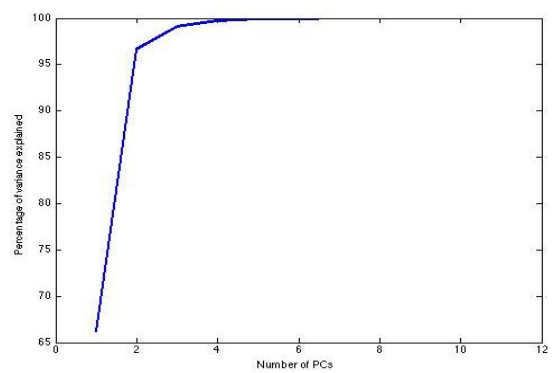

Fig. 5. Accumulative percentage of variance in joint fluid temperature and void fraction simulation data explained by different numbers of PCs.

In Bayesian calibration, the relationship between observed data $\boldsymbol{D}$ and model prediction (or response) $\boldsymbol{M}$ is expressed as [16]

$$\boldsymbol{D} = \boldsymbol{M}(\boldsymbol{x}, \boldsymbol{\theta}) + \delta(\boldsymbol{x}) + \epsilon(\boldsymbol{x}) \tag{3}$$

with $\delta(\boldsymbol{x})$ being a model discrepancy/bias function; ϵ indicating the observation error/uncertainty; $\boldsymbol{x}$ denoting the vector of n_x known variable inputs (pressure, inlet fluid subcooling and wall heat flux) and $\boldsymbol{\theta}$ being the vector of n_θ calibration parameters.

Because tens of thousands of model evaluation would be needed in a typical Bayesian calibration, a less computationally expensive model surrogate (emulator) is needed for $\boldsymbol{M}$. Statistical models for high-dimensional and

multivariate emulator $\boldsymbol{M}(\boldsymbol{x},\boldsymbol{\theta})$ and discrepancy $\delta(\boldsymbol{x})$ were built in this study using a process convolution technique as described in [15,16]:

$$\boldsymbol{M}(\boldsymbol{x},\boldsymbol{\theta}) = \sum_{i=1}^{n_{pc}} \mathbf{k}_i\, \omega_i(\boldsymbol{x},\boldsymbol{\theta}) + \boldsymbol{e} \qquad (4)$$

where { $\mathbf{k}_i$ } is a collection of orthogonal basis vectors obtained as a result of PCA, $\omega_i(\boldsymbol{x},\boldsymbol{\theta})$ are the weights defined over input space, n_{pc} is the number of PCs used to capture all significant variances, and $\boldsymbol{e}$ is an error term accounting for the "noise" effect of omitted PCs.

Each weight ω_i is assumed to be a zero-mean Gaussian process and expressed as $\omega_i(\boldsymbol{x},\boldsymbol{\theta}) \sim \mathcal{N}[0,\, c_{\omega i}((\boldsymbol{x},\boldsymbol{\theta}),(\boldsymbol{x}',\boldsymbol{\theta}'))]$ where the covariance function c_ω is defined as

$$c_{\omega i}((\boldsymbol{x},\boldsymbol{\theta}),(\boldsymbol{x}',\boldsymbol{\theta}')) = \lambda_{\omega i}^{-1} \prod_{l=1}^{n_x} \rho_{\omega i,l}^{4(x_l - x_l')^2} \prod_{k=1}^{n_\theta} \rho_{\omega i,k+n_x}^{4(\theta_k - \theta_k')^2} \qquad (5)$$

with the control hyperparameters $\lambda_{\omega i}$ (precision) and $\rho_{\omega i}$ (correlation length) to be defined (together with $\boldsymbol{\theta}$) in the calibration process.

1D model bias/discrepancy $\delta(\boldsymbol{x})$ can be constructed as a linear combination of limited number of normal kernels placed at equidistant locations along the pipe. A preliminary study conducted in this work (using 5 normal kernels) indicated that the discrepancies were in the bounds of the order 0.001 for void fraction and 10^{-6} for bubble diameter. Consequently, discrepancy was not considered in the following analysis.

$\epsilon(\boldsymbol{x})$ was assumed to be normally distributed and have a zero mean, i.e. $\epsilon(\boldsymbol{x}) \sim \mathcal{N}[0,\, c_\epsilon(\boldsymbol{x},\boldsymbol{x}')]$, with c being the covariance function. In this analysis, $\epsilon(\boldsymbol{x})$ was modeled as homogeneous Gaussian white noise.

Following the Bayes theorem, the posterior distributions of parameters $\boldsymbol{\theta}$ can be computed as follows:

$$\pi(\boldsymbol{\theta}|\boldsymbol{D},\boldsymbol{S}) \propto \mathcal{L}(\boldsymbol{D},\boldsymbol{S}|\boldsymbol{\theta})\pi(\boldsymbol{\theta}) \qquad (6)$$

where $\pi(\boldsymbol{\theta})$ is the prior probability distribution of $\boldsymbol{\theta}$ (taken to be uniform on the ranges of TABLE II) and $\mathcal{L}(\boldsymbol{D},\boldsymbol{S}|\boldsymbol{\theta})$ is the "likelihood" of the observation $\boldsymbol{D}$ and simulation data $\boldsymbol{S}$ (used to construct the emulator) given specific values of $\boldsymbol{\theta}$.

Given the above assumptions about the distributions of data, observation error, and model discrepancy, the 'likelihood' function viewed as a function of ($\boldsymbol{D}$, $\boldsymbol{S}$) is a normal probability density function defined as

$$\mathcal{L}(\boldsymbol{D},\boldsymbol{S}|\boldsymbol{\theta}) \propto \exp\left[-\frac{1}{2}(\boldsymbol{D}^{\mathrm{T}}\boldsymbol{S}^{\mathrm{T}})\boldsymbol{V}^{-1}(\boldsymbol{D}^{\mathrm{T}}\boldsymbol{S}^{\mathrm{T}})^{\mathrm{T}}\right] \qquad (7)$$

with $\boldsymbol{V}$ being a matrix which combines the variance and covariance matrices of $\boldsymbol{M}$, δ and ϵ to give the covariance matrix of the collection of observation and simulation data ($\boldsymbol{D}$, $\boldsymbol{S}$).

Posterior distributions of parameters and hyperparameters were sampled with MCMC. With the model (and statistical model) parameters determined, predictions with the calibrated model can be generated at any new inputs (pressure, inlet subcooling, and wall heat flux).

The GPMSA toolbox was set up to enable model calibration with cross-correlated multivariate datasets, i.e. 1D void fraction & fluid temperature distributions and bubble departure diameter. Cross-covariance was accounted for empirically through PCA on the combined datasets.

III.C. Results and Discussions

Void fraction and fluid temperature data were assumed to be correlated and considered to be of similar type since they described the distributions of variables over a common grid of 1D spatial locations. In the analysis, the void fraction and fluid temperature simulation data sets were separately centered and scaled, then stacked to create a single matrix of simulated output to which PCA was applied. The result of the PCA applied to the combined void fraction and fluid temperature predictions indicated that up to 99.9 % of variance can be captured by the first 6 principal components (PCs). The subsequent analyses utilized 6 PCs (Fig. 6).

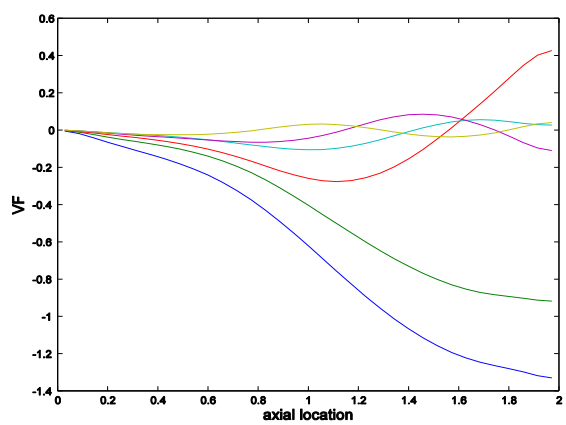

Fig. 6. Variation of void fraction captured by 6 PCs (1-blue; 2-green; 3-red; 4-cyan; 5-purple; 6-brown).

Data on bubble departure diameter were notably different from void fraction and fluid temperature data, since they characterized the dependency of bubble departure size on local subcooling temperature instead of spatial location. Therefore, experimental and simulation data on bubble departure diameter were assumed to be conditionally (given $\boldsymbol{\theta}$) independent of the void fraction and fluid temperature data.

With the standard deviations of void fraction, fluid temperature, and bubble departure size assumed to be 0.06, 2.0 K, and 0.01 mm, respectively, parameters calibration

was conducted as previously described with the results shown in Figs. 8-9.

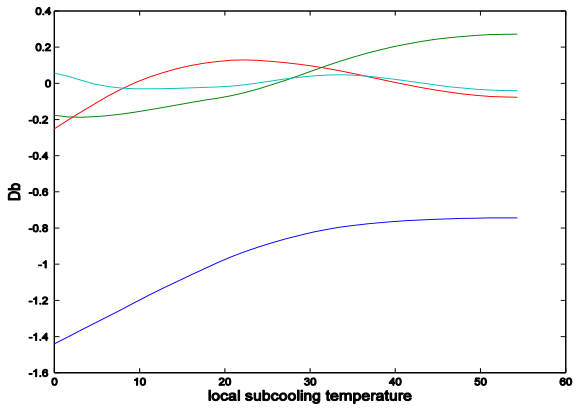

Fig. 7. Variation of bubble departure diameter captured by 4 principal components (1-blue; 2-green; 3-red; 4-cyan).

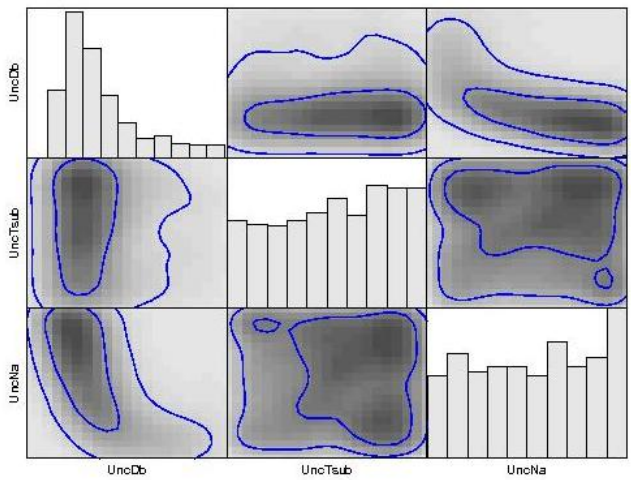

Fig. 8. Posterior distributions of the calibration parameters (d_0-UncDb, ΔT_{ref}-UncTsub, $\bar{N}_a$-UncNa) – Analysis without using data on bubble departure diameter.

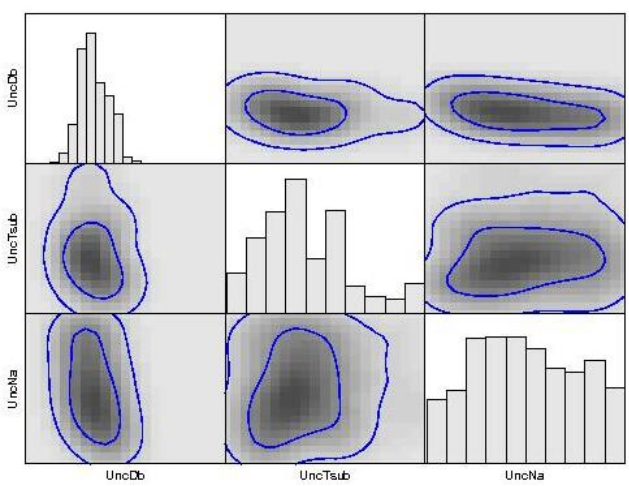

Fig. 9. Posterior distributions of the calibration parameters – Analysis with using data on bubble departure diameter.

Relative insensitivity of the outputs to parameter ΔT_{ref}(UncTsub) could be seen and was manifested in the wide spread in the marginal posterior distributions for this parameter and its weak correlation with other parameters.

The analysis also indicated that additional data on bubble departure diameter could be successfully employed together with other-type data on void fraction and fluid temperature, leading to significantly less spreads in posterior distributions of the calibration parameters.

Calibrated model predictions shown in Figs. 10-13 were obtained by propagating posterior samples of parameters $\boldsymbol{\theta}$ (Fig. 9) through the multivariate emulator $\boldsymbol{M}(\boldsymbol{x},\boldsymbol{\theta})$ for each experimental condition given in TABLE I. These predictions did not account for discrepancy, which was found to be relatively insignificant in a similar analysis by Bui et al. [1].

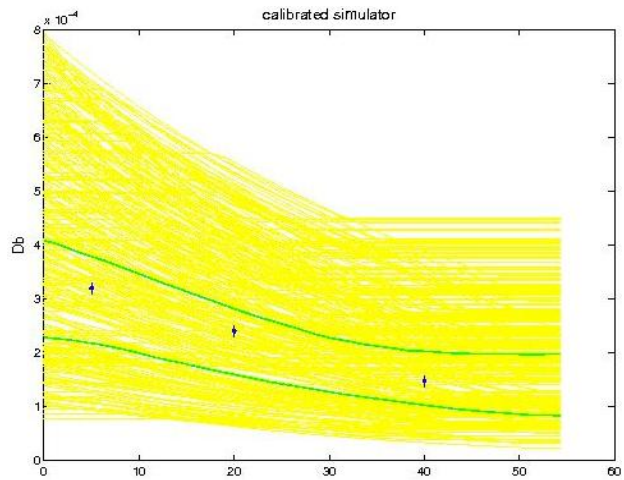

Fig. 10. Prediction of bubble departure diameter with calibrated statistical model. Yellow traces represent simulation outputs and green lines designate the pointwise 90% calibrated prediction interval.

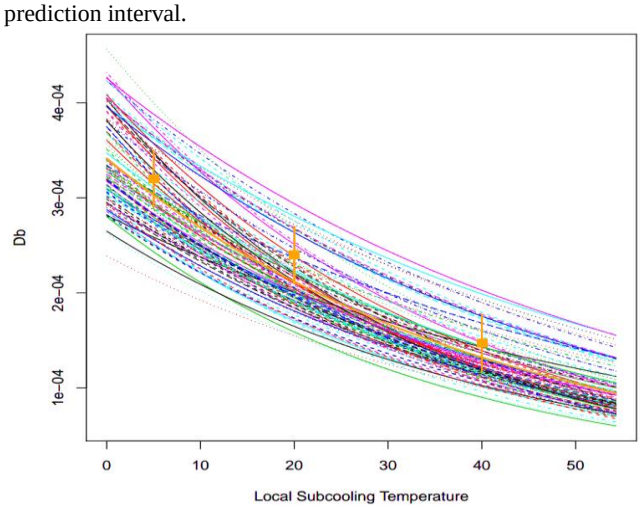

Fig. 11. Spread of bubble departure diameter calculated with Tolubinsky & Konstanchuk's correlation and calibrated parameters. Observed data are shown as red dots with plus/minus three standard deviations ($\pm 3\sigma$).

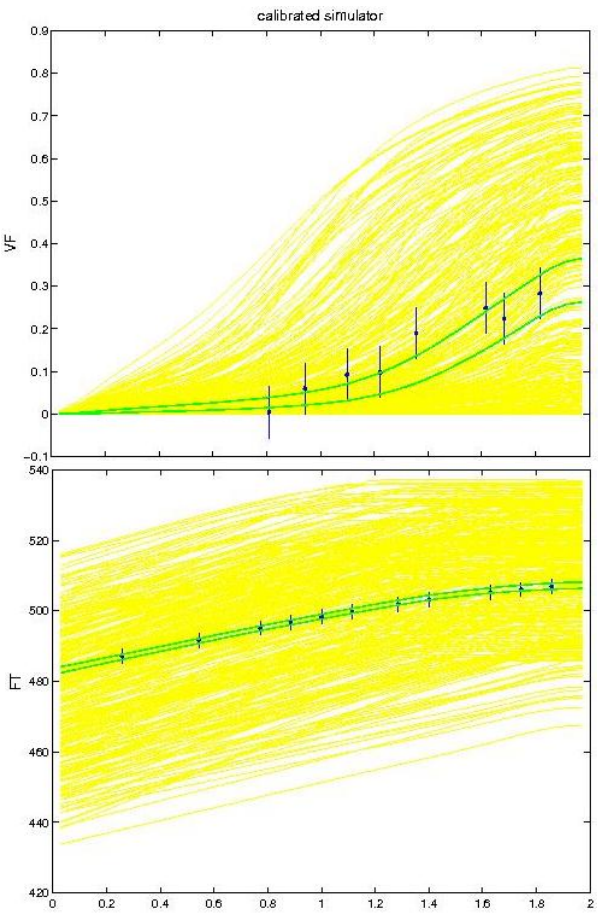

Fig. 12. Prediction of experiment 1 (TALBE I) with calibrated model (top-void fraction, bottom-fluid temperature). Observed data are shown as blue dots with plus/minus one standard deviations ($\pm\sigma$).

It is constructive to note that the construction of a surrogate (statistical) model to represent a simple model such as the bubble departure diameter model is generally unnecessary, since it does not require extensive computational resource and time for evaluation and can be used directly in the calibration process. GPM/SA can be modified to accommodate such a hybrid usage of statistical and real physical models in Bayesian model calibration and validation.

IV. CONCLUSIONS

In the practice of engineering computer model calibration and validation, validation data quality and availability are of great concerns. Measurement data are especially scarce for nuclear power systems either operating under "normal" high-pressure, high-flow rate, high-heat flux operating conditions or involved in accident with possible reactor damage and core melt-down. Data on such complex systems involving many interacting physics may be scarce, of varying quality, and even missing, which complicate the calibration and validation of computer models for system simulation. Better use of a great variety of available data in comprehensive model calibration and validation is therefore essential in the development of next-generation reactor modeling software.

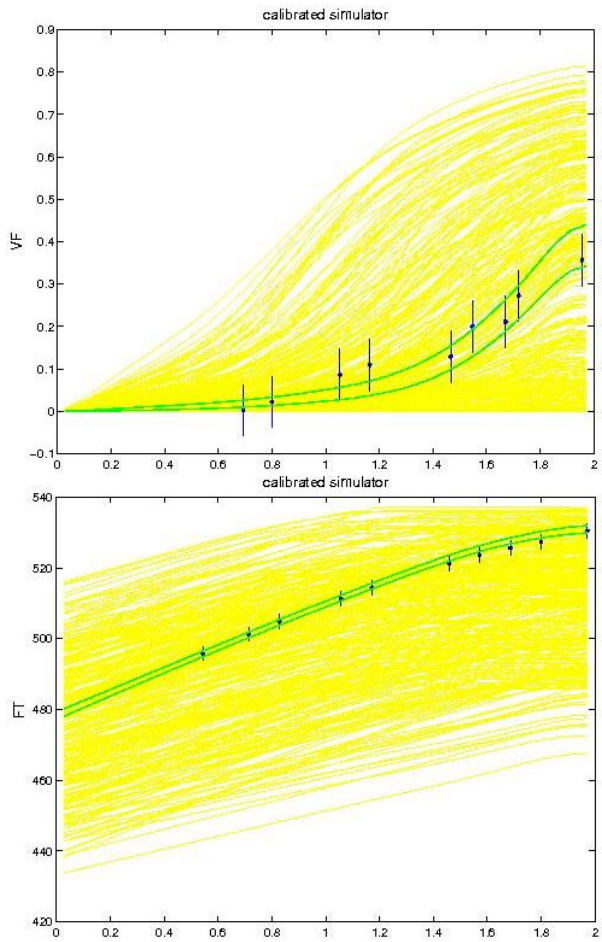

Fig. 13. Prediction of experiment 4 (TALBE I) with calibrated model (top-void fraction, bottom-fluid temperature).

This work demonstrates a new realization of the "total model-data integration" concept to allow assimilation of heterogeneous multivariate data in comprehensive calibration and validation of complex multiphysics models. As shown in this study, the new approach permits simultaneous calibration of submodel parameters, identification of overall model bias/inadequacy and validation of all involved models and submodels.

The new approach leverages on the modern statistical modeling techniques and Bayesian inference to make possible the full usage of data from different sources, of different quality and uncertainty in model calibration/validation and the quantification of uncertainty in model predictions.

ACKNOWLEDGMENT

This research has been supported by the Consortium for Advanced Simulation of Light Water Reactors (http://www.casl.org), an Energy Innovation Hub (http://www.energy.gov/hubs) for Modeling and Simulation of Nuclear Reactors under U.S. Department of Energy Contract No. DE-AC05-00OR22725.

REFERENCES

1. A. Bui, B. Williams, N. Dinh, and R. Nourgaliev, "Statistical Modeling Support for Calibration of a Multiphysics Model of Subcooled Boiling Flows", *Proc. of the Int Conf on Math and Comput Methods Applied to Nucl Sci & Eng (M&C 2013), paper 7464,* Sun Valley, Idaho, USA (2013).

2. M. Ishii and T. Hibiki, "*Thermo-Fluid Dynamics of Two-Phase Flow*", Springer (2010).

3. T. Hibiki and M. Ishii, "One-Dimensional Drift-Flux Model and Constitutive Equations for Relative Motion between Phases in Various Two-Phase Flow Regimes", *Int J Heat Mass Transfer,* **46,** 4935-4948 (2003).

4. A. Bui and N. Dinh, "Quantification of Data Needs, Data Collection and Characterization to Support Validation and Calibration of Subcooled Flow Boiling Model", *INL Tech Report, INL/EXT-13-28709* (2013).

5. V. Dhir, H. Abarajith and D. Li, "Bubble Dynamics and Heat Transfer During Pool and Flow Boiling", *Heat Transfer Eng,* **28,** 608-624 (2007).

6. V. I. Tolubinsky and D. M. Konstanchuk, "Vapour Bubbles Growth Rate and Heat Transfer Intensity at Subcooled Water Boiling Heat Transfer", *Proc. of the 4th Int Heat Transfer Conf, paper B-2.8,* Paris, France (1970).

7. R. Cole, "A Photographic Study of Pool Boiling in the Region of the Critical Heat Flux", *AIChE J,* **6**, 533-542 (1960).

8. M. Lemmert and J.M. Chawla, "Influence of Flow Velocity on Surface Boiling Heat Transfer Coefficient", in "*Heat Transfer in Boiling*", 237-247, Hemisphere Publ. Company (1977).

9. N. Kurul and M. Podowski, "Multidimensional Effects in Forced Convection Subcooled Boiling", *Proc. of the 9th Int Heat Transfer Conf,* Jerusalem, Israel (1990).

10. G. Bartolomej and V. Chanturiya, "Experimental Study of True Void Fraction When Boiling Subcooled Water in Vertical Tubes", *Thermal Engineering*, **14**, 123-128 (1967).

11. G. Kocamustafaogullari, "Pressure Dependence of Bubble Departure Diameter for Water", *Int Comm Heat Mass Transfer*, **10**, 501-509, 1983.

12. J. Gattiker, "Gaussian Process Models for Simulation Analysis (GPM/SA) - Command, Function, and Data Structure Reference," *LANL Tech Report* (2008).

13. B. Adams, W. Bohnhoff, K. Dalbey, J. Eddy, M. Eldred, D. Gay, K. Haskell, P. Hough and L. Swiller, "DAKOTA, A Multilevel Parallel Object-Oriented Framework for Design Optimization, Parameter Estimation, Uncertainty Quantification, and Sensitivity Analysis: Version 5.0 Reference Manual," *Sandia Tech Report, SAND2010-2184* (2013).

14. I. Jolliffe, "*Principal Component Analysis"*, Springer (2002).

15. H. Lee, C. Holloman, C. Calder and D. Higdon, "*Flexible Gaussian process via convolution*", Duke University (2002).

16. D. Higdon, M. Kennedy, J. Cavendish, J. Cafeo and R. Ryne, "Combining field data and computer simulations for calibration and prediction," *SIAM J Sci Comput,* **26**, 448-466 (2004).